SSCL-496

SSCL-496

Superconducting Super Collider Laboratory

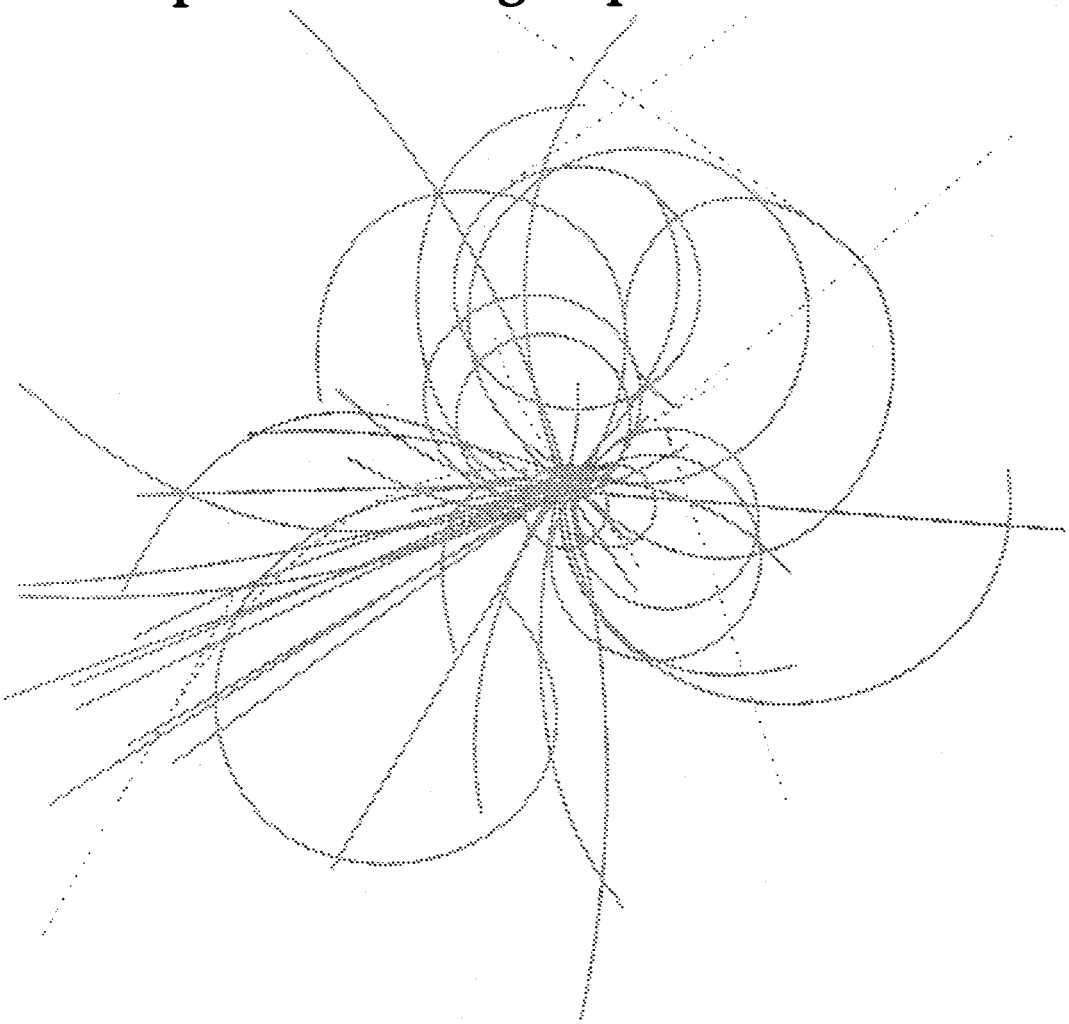

The SSC Access Shafts Calculational Study

I. Baishev, N. Mokhov, and T. Toohig

June 1991

SSCL-496

The SSC Access Shafts Calculational Study

I.S. Baishev, N.V. Mokhov, and T.E. Toohig

Accelerator Divison
Superconducting Super Collider Laboratory†
2550 Beckleymeade Ave.
Dallas, TX 75237

June 1991

† Operated by the Universities Research Association, Inc., for the U.S. Department of Energy under Contract No. DE-AC02-89ER40486.

1.0 INTRODUCTION

The SSC generic shaft requirements and access spacing are considered elsewhere [1]. The shafts connecting the ground surface with the underground accelerator tunnel deliver to the surface some portion of the radiation created in the tunnel [2]. The radiation safety problem of access shafts consists of two major questions:

- does the dose equivalent at the ground surface exceed permissible limits?
- if it exceeds those limits, what additional shielding measures are required?

A few works deal with this problem for high energy machines [3-6]. This work is an attempt to answer these questions for the basic types of shafts specific to the SSC magnet delivery, utility and personnel shafts using full-scale Monte-Carlo calculations of the entire process from hadronic cascades in the lattice elements to particles scattered in the tunnel, niches, alcoves, shafts and surface bunkers and buildings.

2.0 BEAM LOSS

Beam loss and the corresponding radiation effects in the SSC lattice elements have been considered in paper [2] for all the expected sources. In the present paper the beam intensity is assumed to be 4×10^{14} in each ring. For design purposes the beam loss in the vicinity of shafts is supposed to be 10^5 protons per meter of the lattice per sec in either ring at 20 TeV. This number is derived independently from three conditions:

1) it corresponds to 1/50 of the quench level [2,7] and is the set point for the Beam Loss Monitor (BLM) abort trigger (Tevatron experience), i.e. beam loss at a rate of a little less than 10^5 protons per meter per second can occur at any particular lattice location.
2) it corresponds to the SCDR suggestion - accidental loss of a whole beam once a year at an arbitrary one-half standard cell of the ring.
3) beam loss at such a rate can occur in the SSC magnet elements according to the first full-scale calculations as described in [2].

Of course, one can control the beam loss in specific lattice regions, but at the design stage, we think that the above assumption is reasonable for radiation safety.

3.0 MONTE CARLO CALCULATIONS

Simulation of hadronic and electromagnetic cascades induced by beam loss in the standard cell in the vicinity of the shaft mouth, as well as the subsequent low energy neutron transport are carried out in this work with the newest version of the MARS Monte Carlo system [7-9]—MARS12 code. One of the extended features of MARS12 is a new efficient algorithm for low energy neutron transport which is based on the multi-group neutron cross-section library covering the energy range from thermal up to 14.5 MeV. It includes also photoneutron production, which has a non-zero contribution to the result due to the important role of electromagnetic showers at 20 TeV. Two major components of the radiation fields are mentioned often below: "hadrons," i.e., protons, neutrons and charged pions with energy above 14.5 MeV and "neutrons" i.e., neutrons with energy below 14.5 MeV. The calculational model of the magnet delivery shaft junction is shown in Fig. 1. Figures 2 and 3 show the model of a utility shaft, personnel shaft and the niche junctions. The z-axis of the drawings coincides with the lower beam line axis and the x-axis is directed up to the ground surface. Most of the results presented below are normalized per one 20 TeV beam lost per 1 meter of the standard cell length. Some final results are presented for the beam loss scenario described in Section 2.

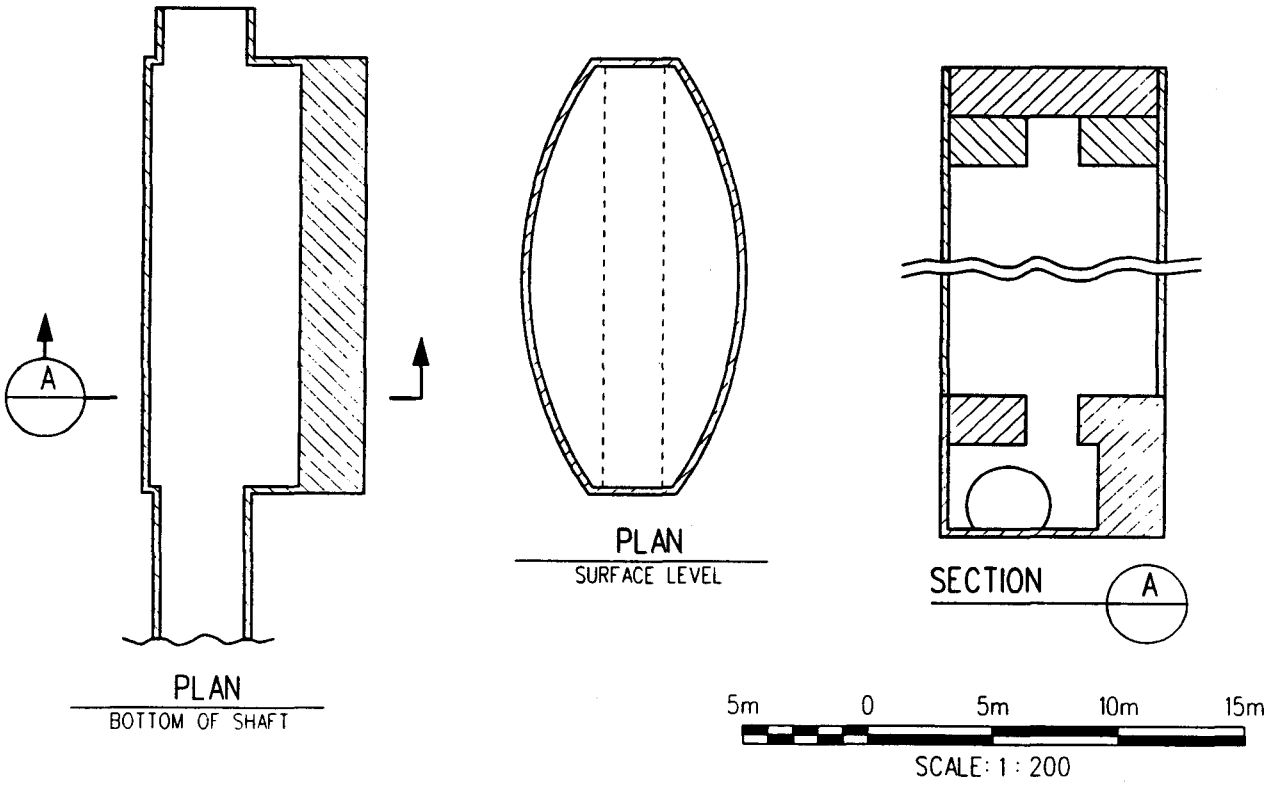

Figure 1. Schematic of the SSC magnet delivery shaft.

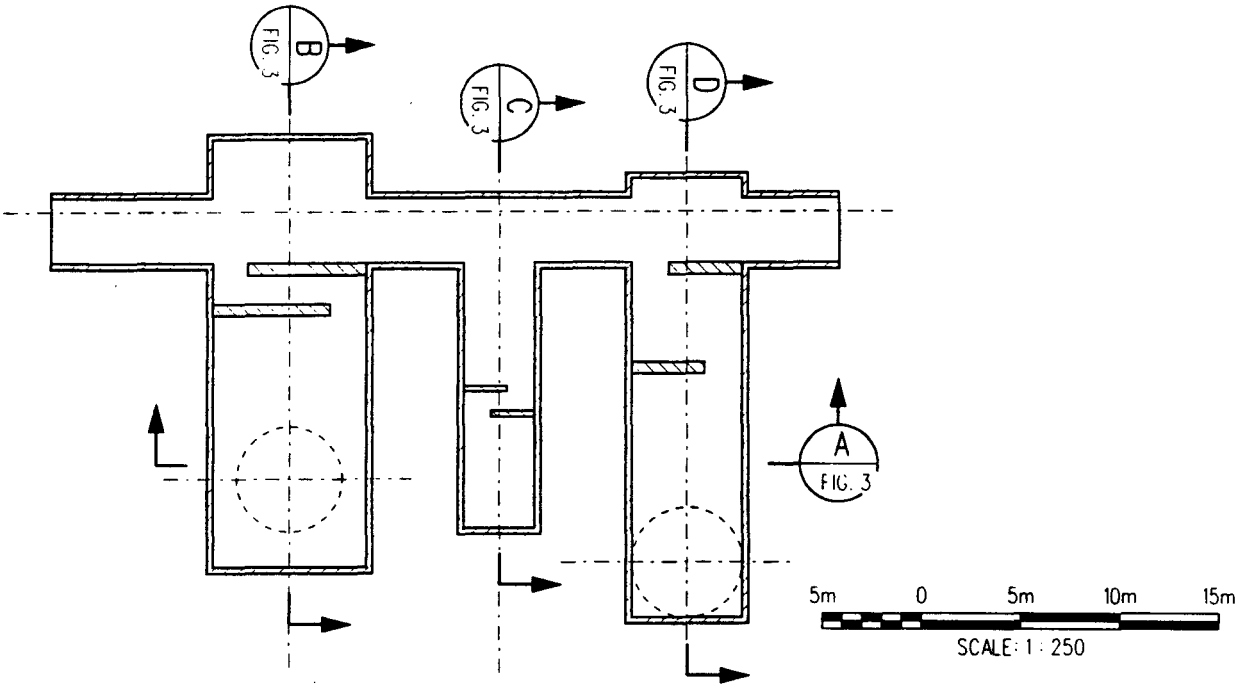

Figure 2. Schematic of the SSC service shaft trident (plan).

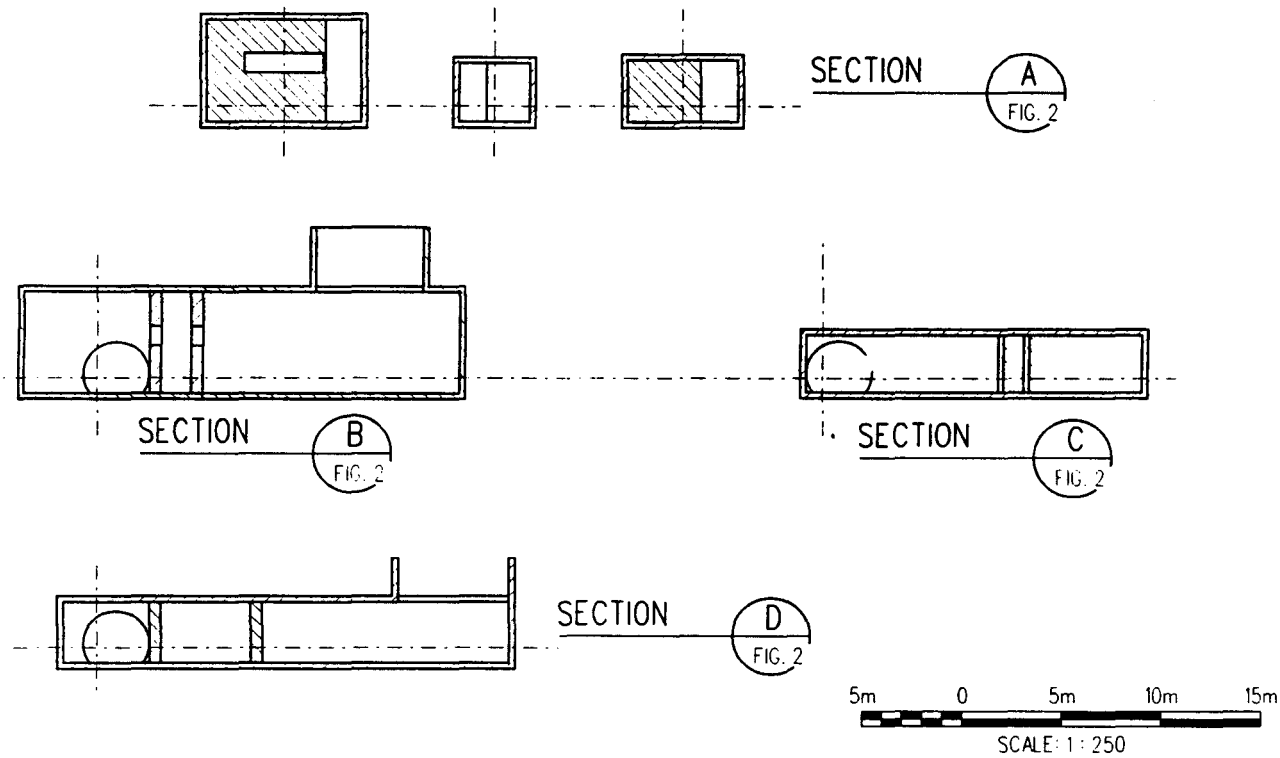

Figure 3. The same, some details in the vertical plane.

4.0 TUNNEL

Figure 4 shows the fluences of hadrons and neutrons as a function of the distance from the beam axis in the tunnel cross-section. Low-energy neutron fluence is about one order of magnitude higher and falls off much more slowly as compared to hadrons. Particle spectra in the high energy and low energy regions are presented in Figs. 5 and 6 at the superconducting magnet surface and at 70 cm distance from the beam. There is one peak in the charged hadron spectra around 300 MeV and three peaks in the E × F(E) neutron spectra around 60 MeV, an outstanding 1 MeV peak, and a thermal neutron peak.

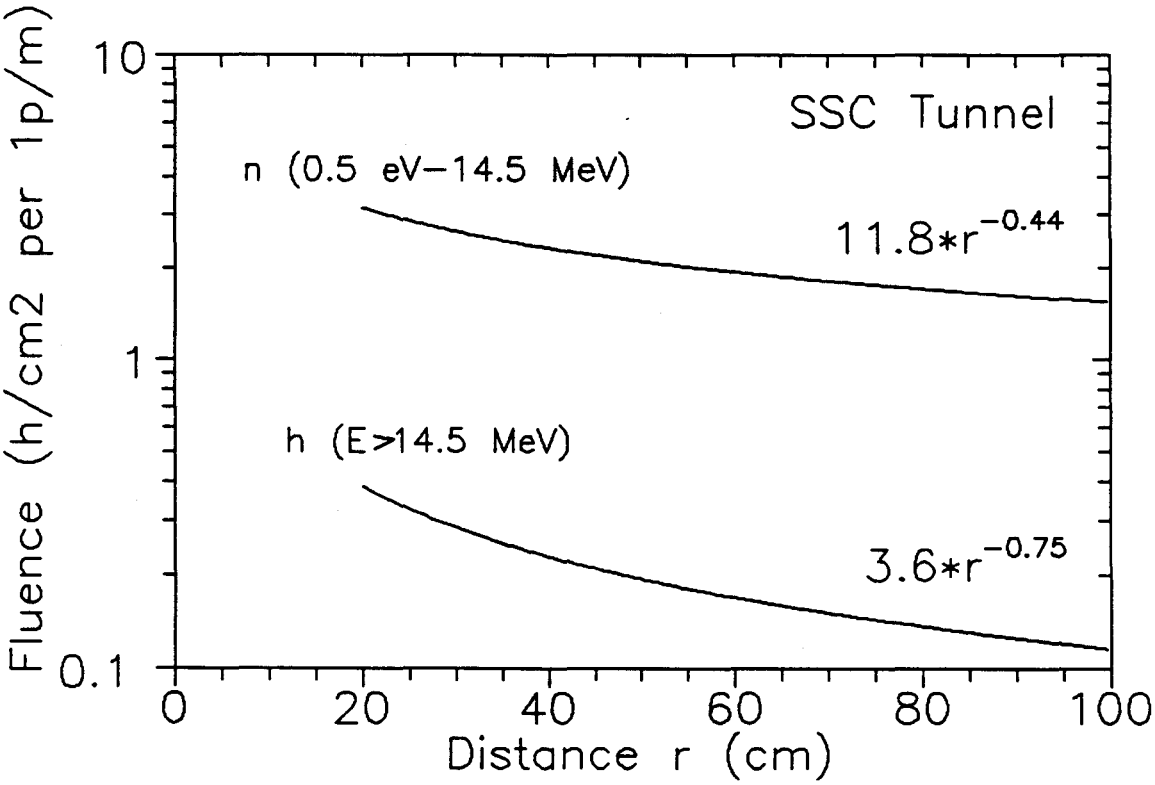

Figure 4. Fluence of hadrons and low energy neutrons in the SSC tunnel versus distance from the TeV beam centerline.

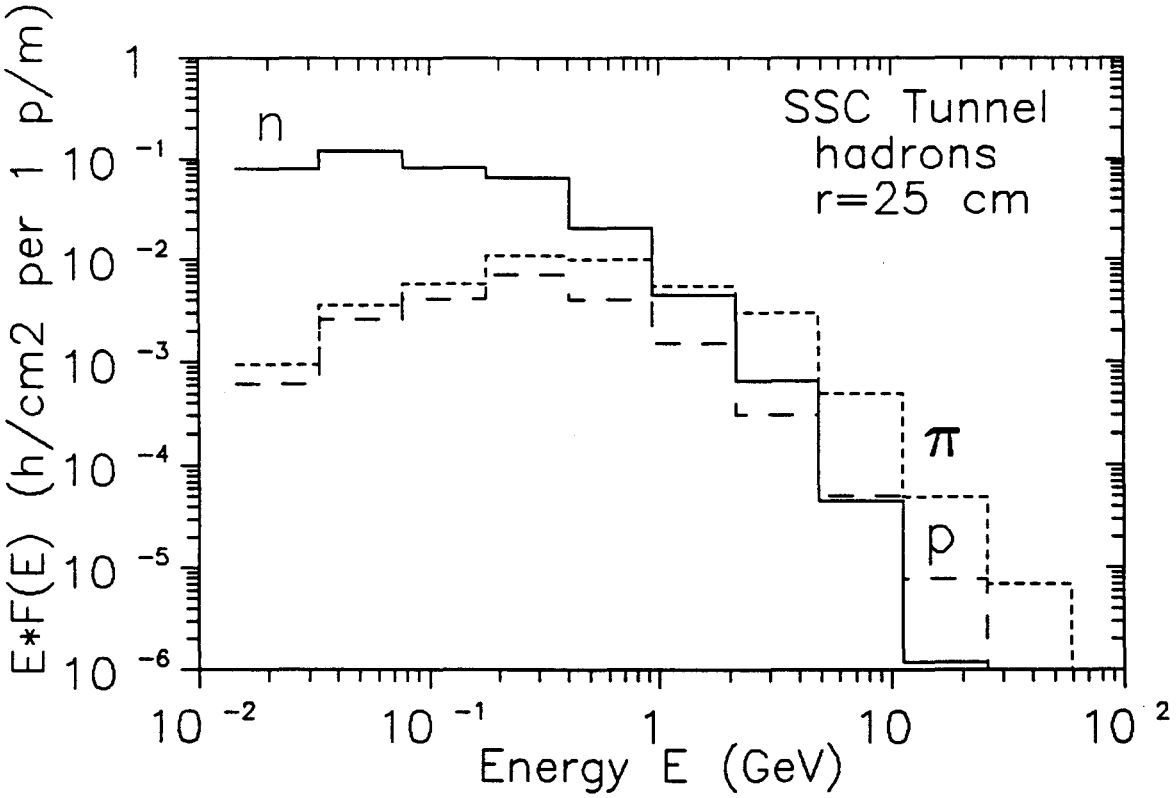

Figure 5. Energy spectra of hadrons at the surface of the SSC dipoles.

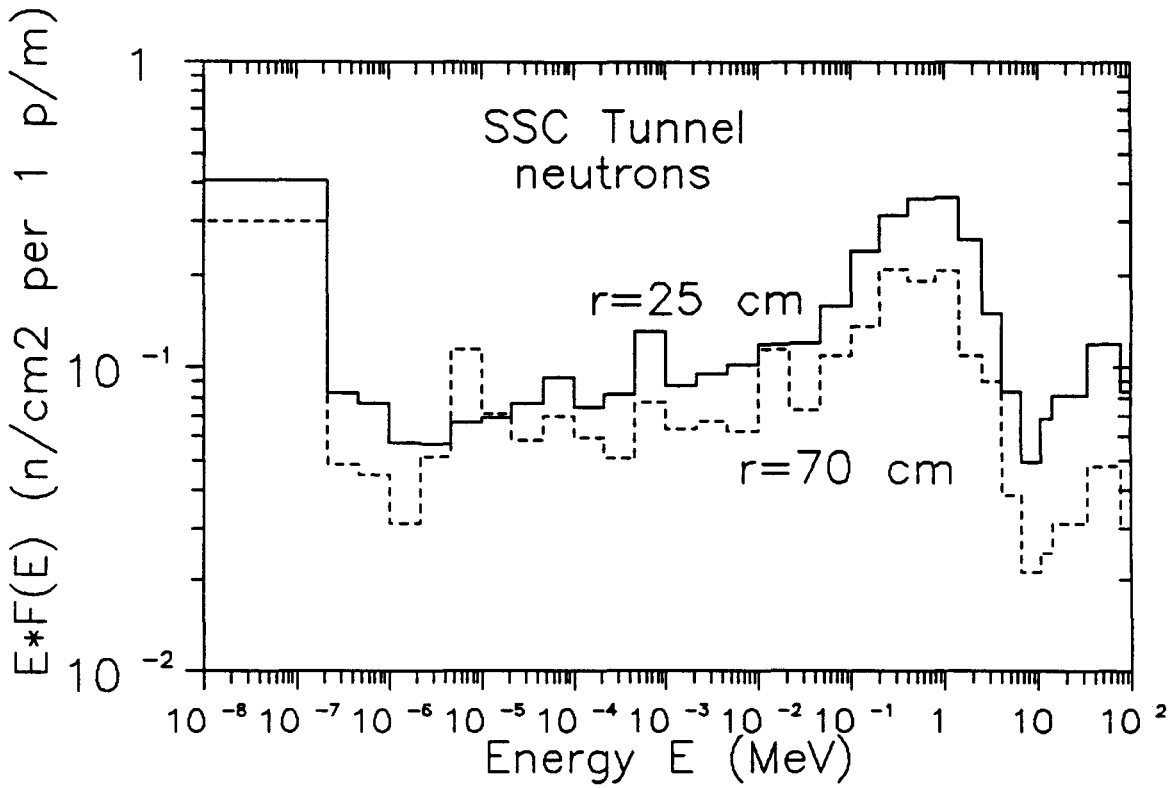

Figure 6. Energy spectra of neutrons in the SSC ring at two distances from the beam centerline.

5.0 MAGNET DELIVERY SHAFTS

From the radiation safety point of view the magnet delivery shaft is the most difficult of the SSC shafts. Its vertical axis is very close to the beam axis. The proposed 25 foot concrete shield underneath the shaft mouth cannot properly attenuate radiation because of the wide (8 feet) slot in it. Figure 7 shows the dose attenuation in the slot which is very slow compared to the attenuation in solid concrete (at least one order of magnitude per one meter). One can propose, therefore to reduce the lower shielding thickness to approximately 2 meters. The neutron energy spectra in the shafts are much softer than the ones in the tunnel (Fig. 8). To a first approximation they behave as $E \times F(E) = \text{const}$ below a few MeV in the first 10–30 meters of the vertical shaft. At the larger distances the spectra become softer.

Dose attenuation in the shaft itself is presented in Figure 9 as a "universal curve," where L is a distance from the shaft mouth and S is the shaft cross-sectional area. It is interesting that the results are in good agreement with the "universal curve" given in [4] for a linear source. Even for the deepest shaft at E1 the annual dose at the surface in the absence of supplementary shielding reaches 40 Rem. For other delivery shafts it is much higher (600 Rem for F3 shaft). The dose can be easily reduced to the required value by covering the top of each delivery shaft with a concrete cap. Figure 10 shows the attenuation of the high energy hadrons and low energy neutrons in such a shielding. One can notice two components in the neutron fluence: primarily, it is due to low energy neutrons coming from the shaft (this is 1000 times higher than that due to the hadron fluence) and then there is the neutron component generated in the cap by hadrons. The corresponding dose attenuation in a top cap made of ordinary concrete is shown in Fig. 11.

The cap thickness required to reduce annual dose at the surface to 50 mrem is plotted on Figure 12 as a function of the shaft depth to the beamline. To reduce the annual dose to 20 mrem one needs to add another 70 cm of ordinary concrete to the cap. So, caps of thickness 1.7 to 3.7 meters, depending on shaft depth, solve the problem completely.

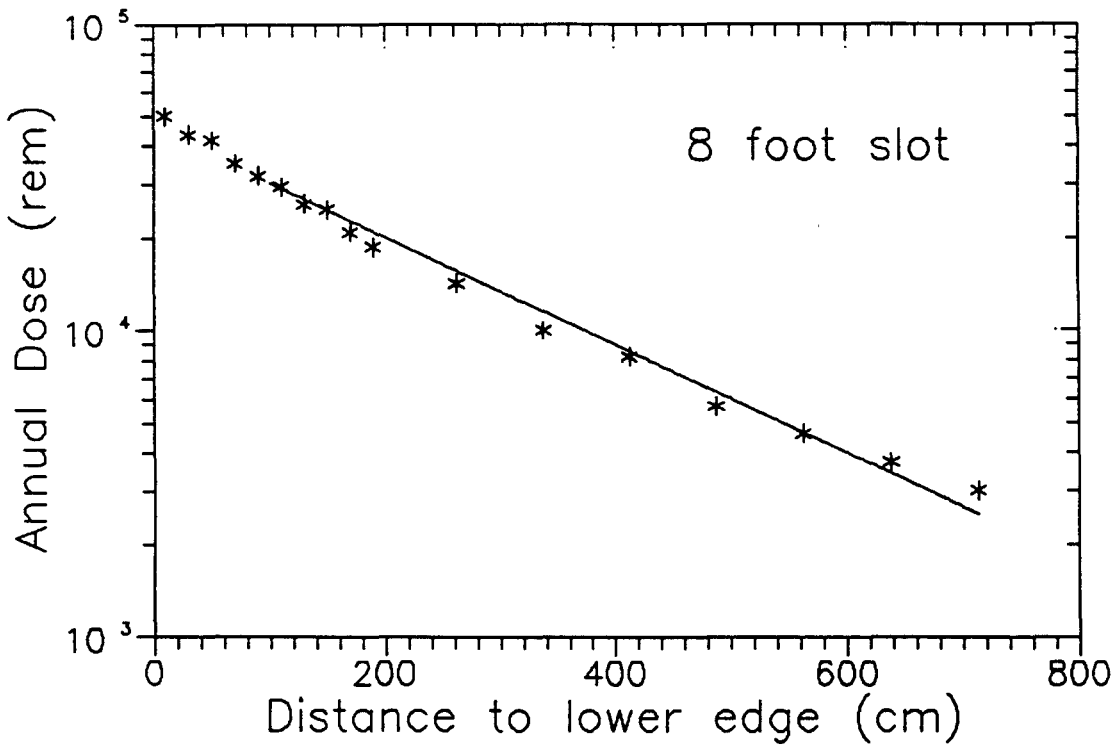

Figure 7. Attenuation of dose equivalent in the 8 foot slot of the lower concrete shielding in the magnet delivery shaft.

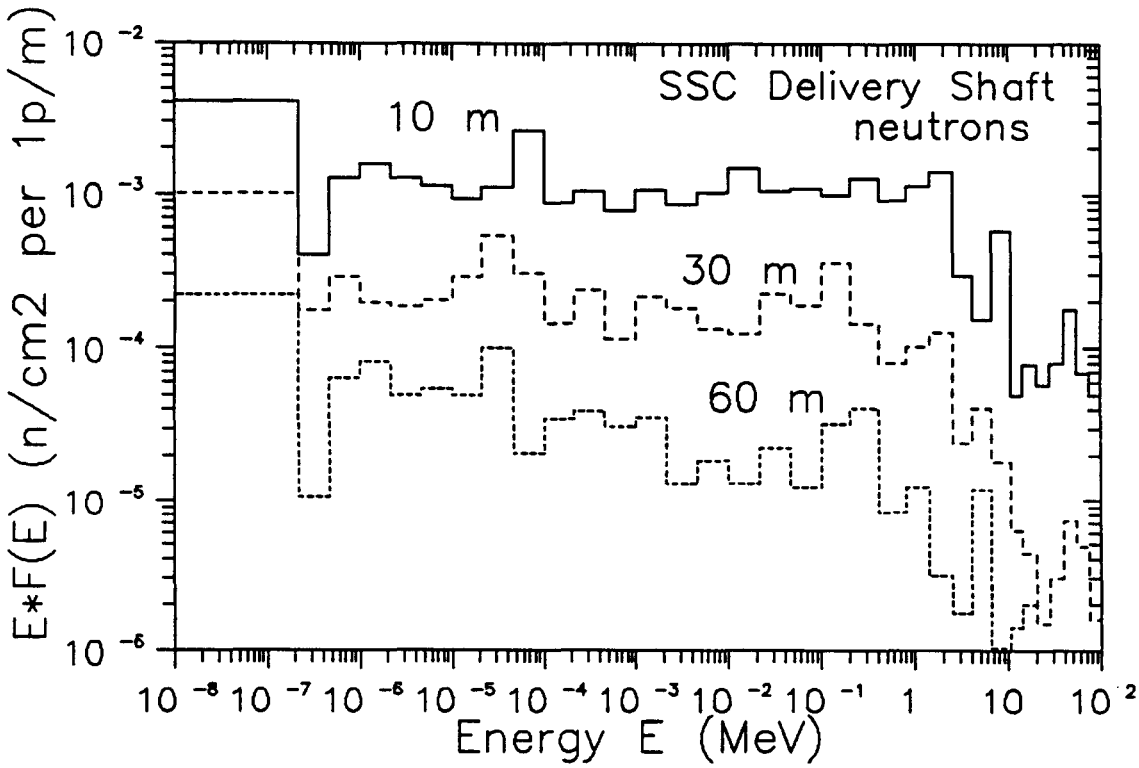

Figure 8. Neutron energy spectra at 3 vertical positions along the delivery shaft.

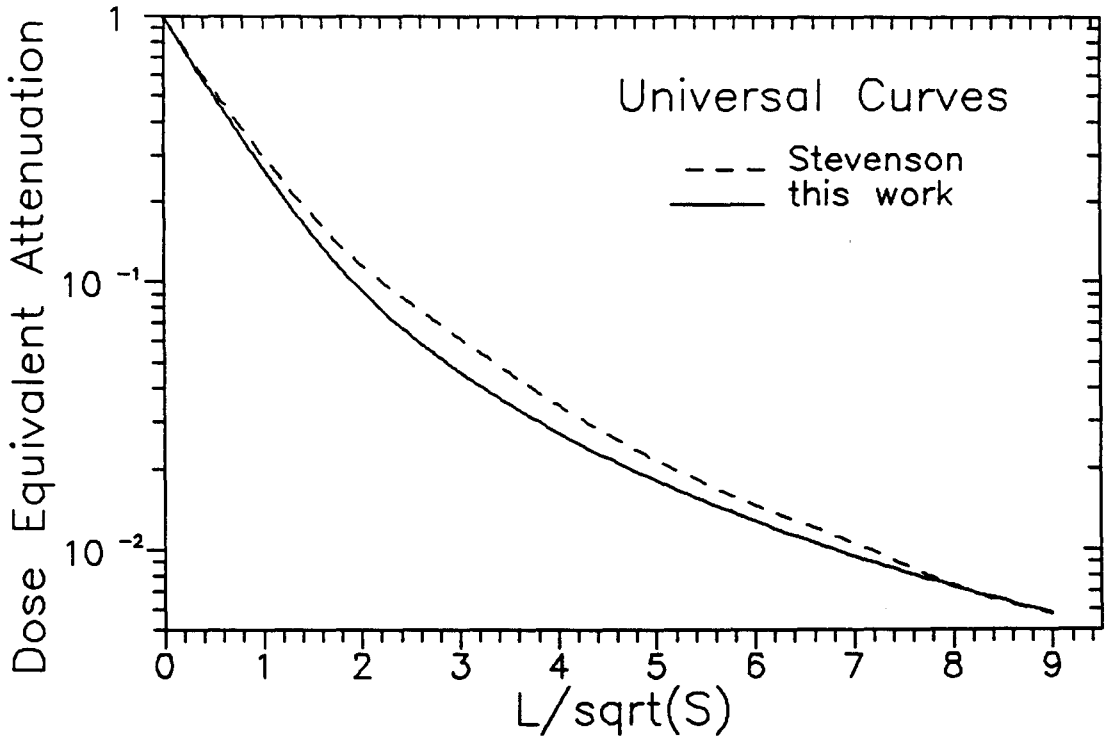

Figure 9. Dose attenuation in the delivery shaft ("labyrinth's first section"). L is a distance from theshaft entrance, S is the shaft cross-section. Also shown is the CERN "universal" curve for the first section.

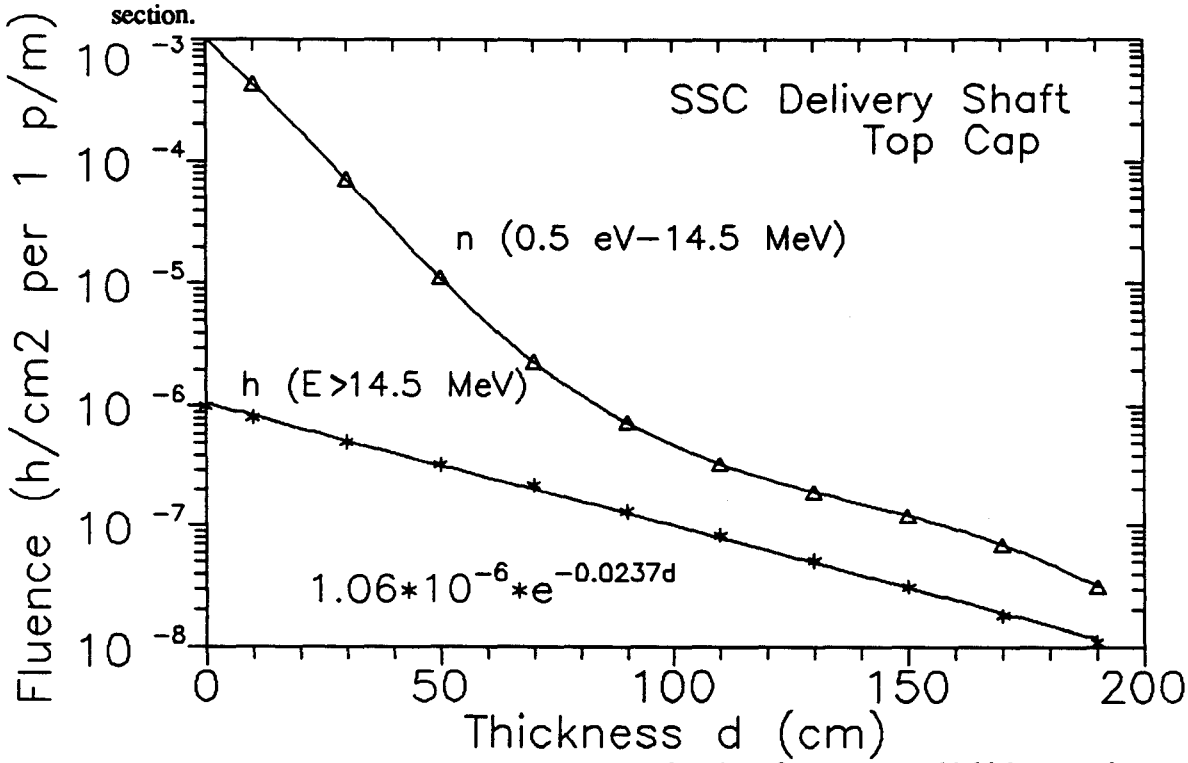

Figure 10. Fluence of hadrons and low energy neutrons as a function of concrete shield thickness at the top of delivery shaft.

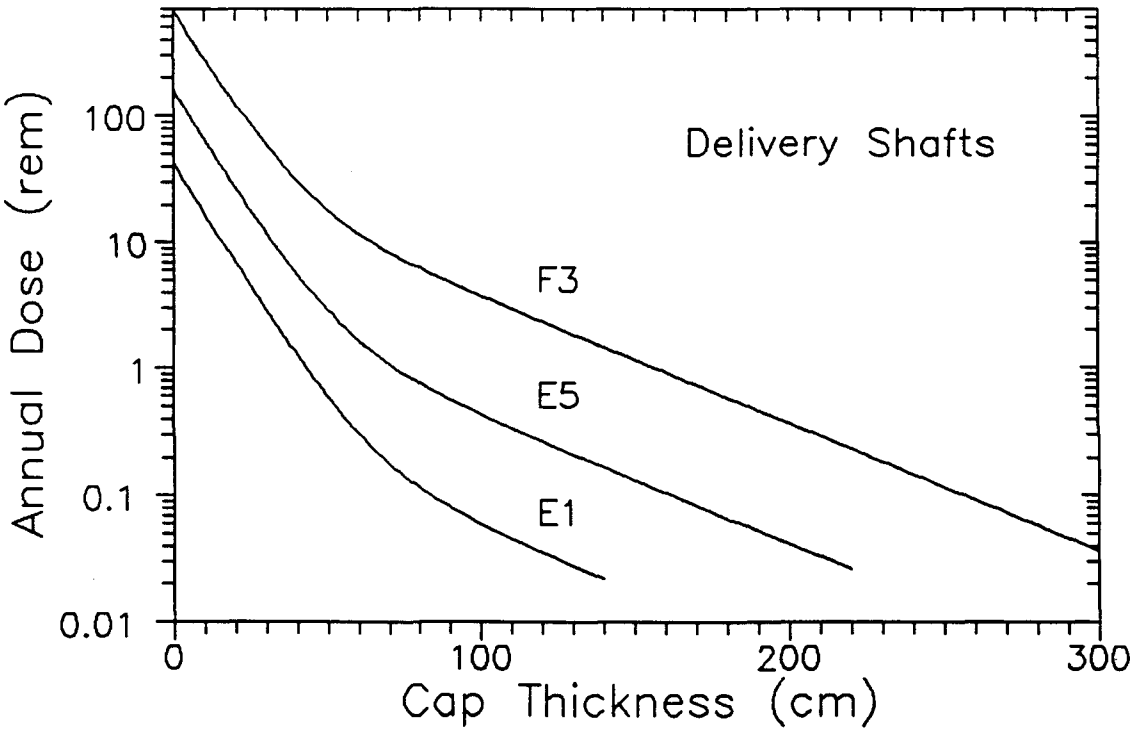

Figure 11. Annual dose at the top of 3 SSC shafts versus concrete cap thickness.

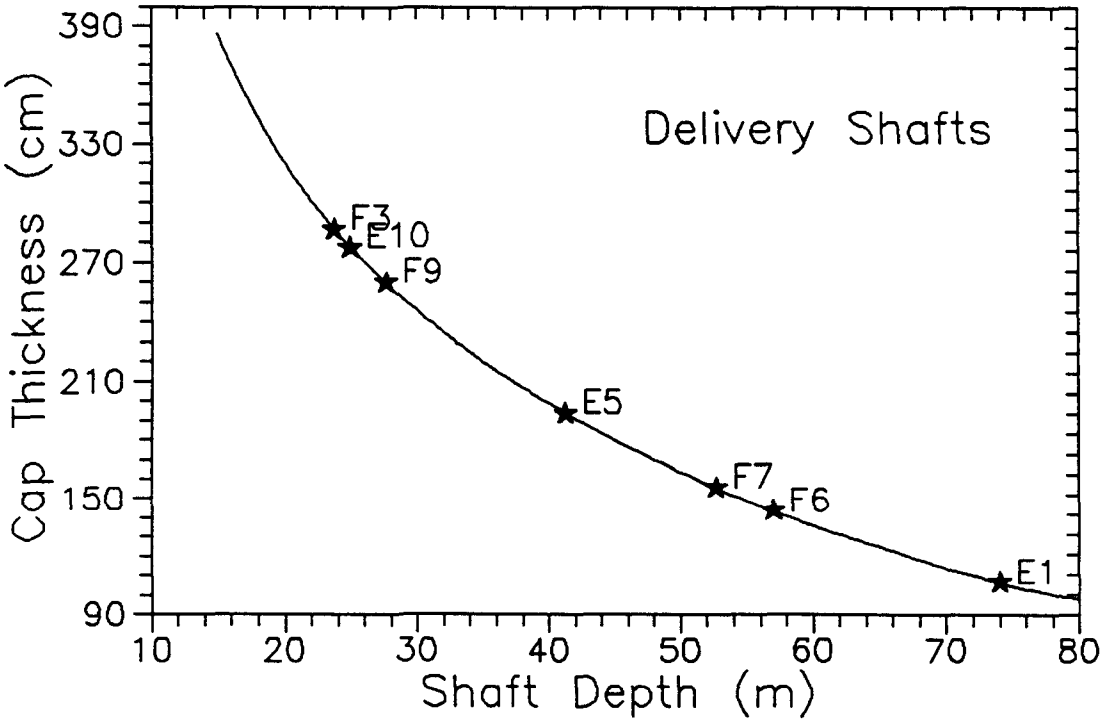

Figure 12. Top concrete shielding thickness required to reduce annual dose to 50 mrem versus shaft depth. To get 10 mrem, additional 70 cm of concrete is required.

6.0 UTILITY SHAFTS

The utility shafts with their alcoves create classical bi-sectional labyrinths. In addition two shielding walls at the beginning of each alcove create another small labyrinth. The attenuation factor of these small labyrinths, i.e., the dose at the shaft mouth related to the dose at the shaft mouth in absence of any shielding walls is shown in Fig. 13 as a function of wall thickness. Sixty cm seems to be the optimum thickness for these walls. The results below are presented for just such a case.

Figure 14 shows the vertical distribution of various energy group fluences in the utility shaft. The corresponding dose attenuation is presented in Fig. 15 as "universal curve" which is in good agreement again with the curve given in [4] for the second section of a labyrinth.

Figure 16 shows the dependence of the annual dose at the ground surface on the shaft depth to the beam axis. As can be seen, the acceptable dose level (20 mrem) is exceeded for all of the shafts, and additional shielding measures have to be taken. These additional measures are a third wall in the alcove, use of boron-content concrete or boron-content sheets at the very top of the shafts, and creation of concrete bunkers above the top of most of the utility shafts.

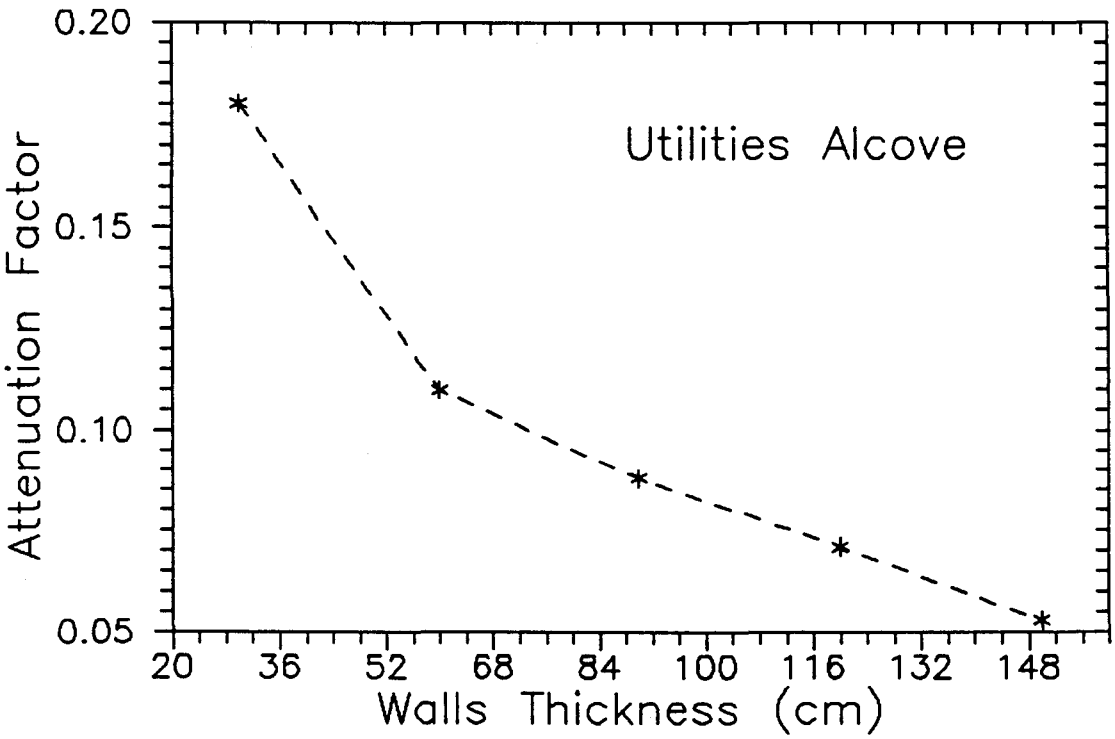

Figure 13. Shielding effect of two concrete walls in the utilities shaft alcove as a function of wall thickness.

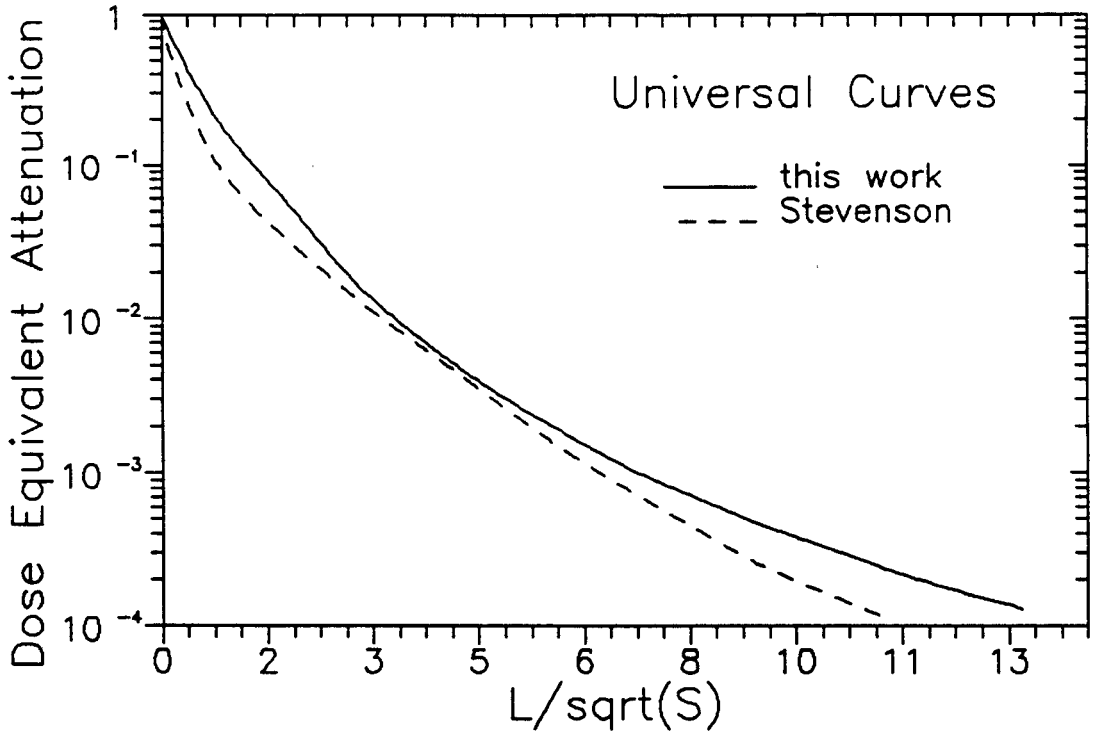

Figure 14. Distributions of hadron and neutron fluences along the vertical utilities shaft. From up to down: total fluence, neutrons (0.5–14.5 MeV), neutrons (E < 0.5 MeV), hadrons (E > 14.5 MeV).

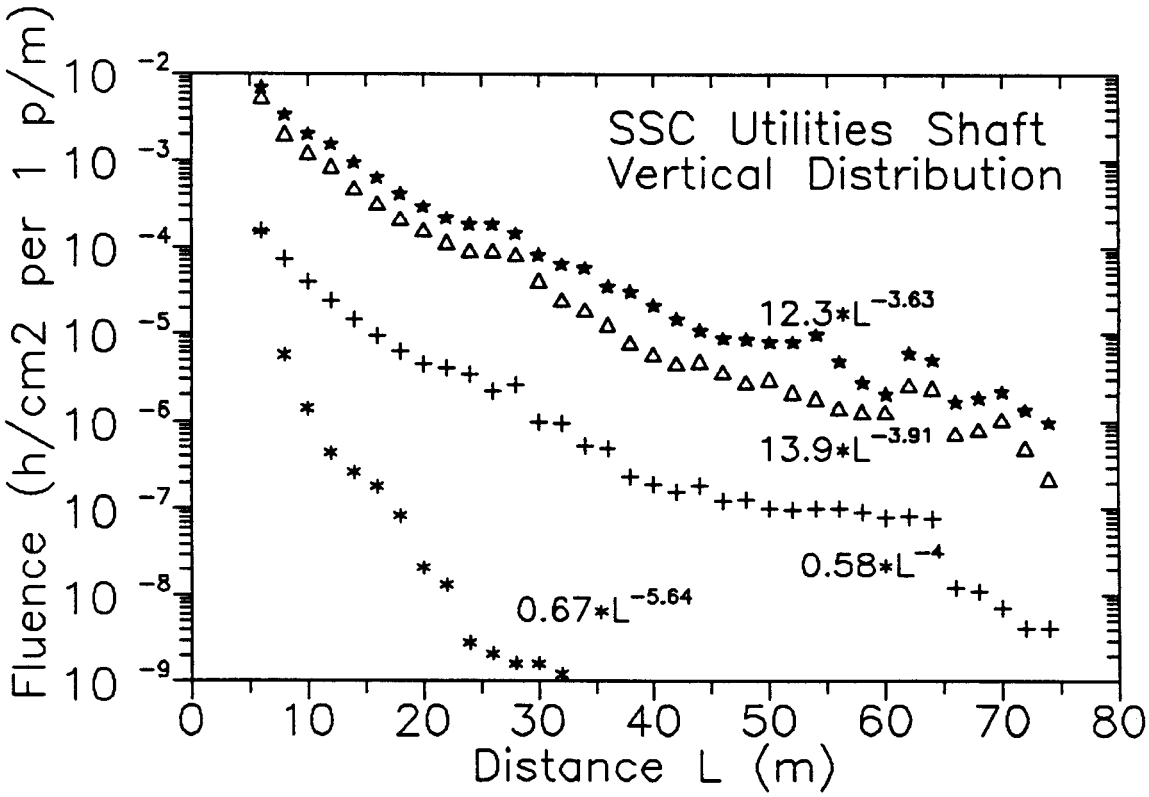

Figure 15. Dose attenuation in the vertical utilities shaft ("labyrinths second section"). Also shown is the CERN second leg "universal curve."

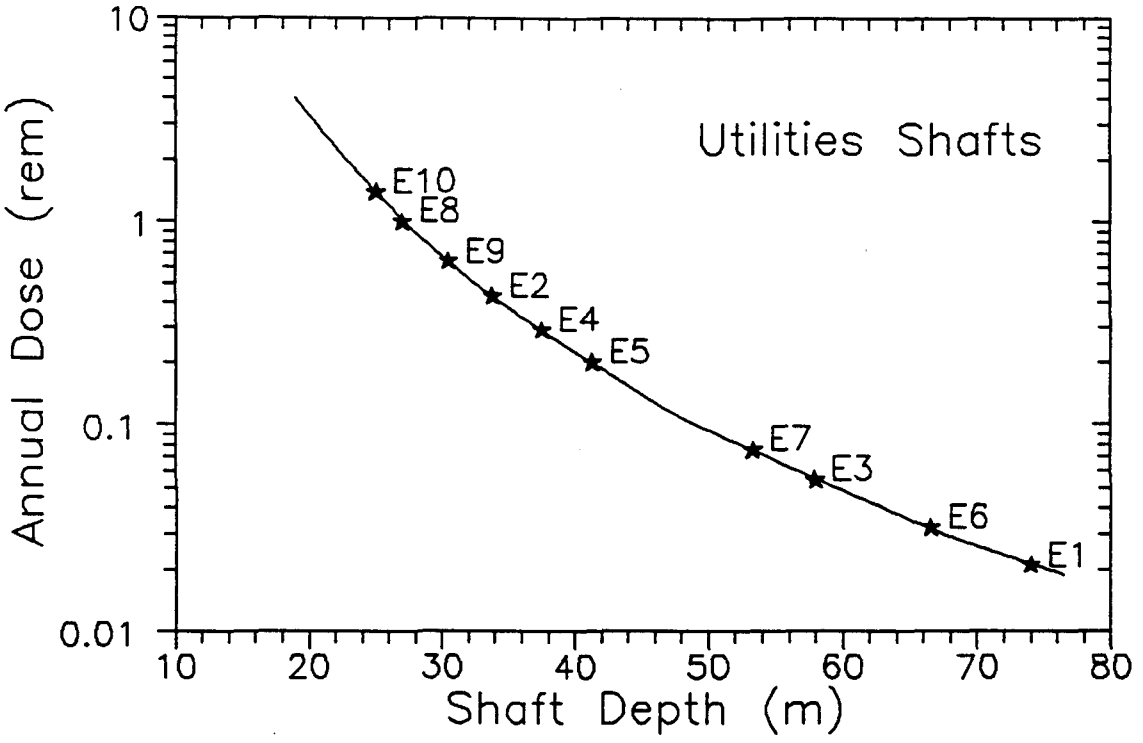

Figure 16. Annual dose at the top of utilities shafts without shielding as a function of shaft depth.

7.0 PERSONNEL SHAFTS

The neutron flux per interacting proton, F_n, in the case of the updated layout of the utility and personnel shafts are:

- utility shaft–Fn = 2×10^{-3}
- personnel shaft–Fn = 2.6×10^{-3}.

The main difference between the two is the absence of holes in shielding walls for the personnel shafts.

There is a question about walls in personnel shafts:

- if there are no real walls, the attenuation along the shaft can be easily estimated using a "universal curve".
- if there are, new runs are necessary.

8.0 RADIATION DAMAGE TO ELECTRONICS AND FIBER OPTICS

All the doses above are given for tissue. The contributions of different components to the energy deposition have a strong influence on such a dose as well as on the dose to other materials at various locations in the region of the shafts. There are two important points of

interest: electronics in niches and fiber optics under the floor. To give a tool for dose estimation in these elements, general fluence and dose characteristics are presented in Table 1. For example, with the results presented in the above sections and the data of the Table, the annual dose to the underfloor fiber optics is estimated to be a few kilorads.

Table 1. Fluence and Dose Characteristics of the Ring Radiation

Value	Tunnel 30 <r<75 cm	Niches, Utility Shaft Vert. Mouth
F(len)/F(h) (=8 at 30 cm, =14 at 75 cm)	11	23
F(ch_h)/F(h)	0.12	~0.08
F(e)/F(ch_h)	2.85	<0.06
Edep(i)/Edep(tot): i		
len	0.05	0.28
ecp	0.12	~0.30
ch h	0.31	~0.40
EMS	0.52	<0.02
D(Si)/F(h), rad*cm^2	2.2×10^{-8}	1.9×10^{-9}
D(Si)/F(len), rad*cm^2	2.0×10^{-9}	8.3×10^{-11}
k(Si), h, rad*cm^2	2.1×10^{-8}	1.4×10^{-9}
k(Si), len, rad*cm^2	8.3×10^{-8}	2.3×10^{11}
D(tiss)/D(Si)	2.8	24
H(tiss)/F(h), rem*cm^2	2.1×10^{-7}	3.0×10^{-7}
H(tiss)/F(len), rem*cm^2	1.9×10^{-8}	1.3×10^{-8}
q(tiss), h, rem*cm^2	7.0×10^{-8}	7.0×10^{-8}
q(tiss), len, rem*cm^2	1.3×10^{-8}	1.0×10^{-8}
<QF>	3.4	6.5

h	hadrons with E > 14 MeV
ch_h	charge hadrons with E > 14 MeV
len	neutrons with 0.5 eV < E < 14 MeV
e	electrons and positrons with E > 1 MeV
ecp	evaporated charge particles (p,fragm.) due to hA int.
EMS	electromagnetic showers
D	total absorbed dose
k	kerma factor
H	total dose equivalent
q	specific dose equivalent

REFERENCES

1. Footprint Characterization Document, SSCL-SR-1041, June 1990.
2. I.S. Baishev, A.I.Drozhdin and N.V. Mokhov. Beam Loss and Radiation Effects in the SSC Lattice Elements, SSCL-306, 1990.
3. H.G. Vogt, CERN 75-14, Geneva, 1975.
4. G.R. Stevenson, CERN 76-04, Geneva, 1976.
5. I.S. Baishev and N.V. Mokhov. On scattered radiation fields in UNK labyrinths. Proc. of 8 Allunion Conference on Charged Particle Accelerator v. **2**, p. 198. Dubna, 1983.
6. I.S. Baishev, N.V. Mokhov et al. On the formation of scattered radiation fields in the labyrinths of proton accelerators. Proc. of 3 Allunion Conf. on Shielding Against Ionizing Radiation.v. **6**, p. 3. Tbilisi, 1985.
7. A.N. Kalinovsky, N.V.Mokhov and Yu.P. Nikitin. Passage of High Energy Particles Through Matter, AIP, New York, 1989.
8. N.V. Mokhov. Sov. J. Part. Nucl. v. **18**(5), pp. 408–426, 1987.
9. N.V. Mokhov. The MARS10 Code System. FN-509, Fermilab, 1989.